Available online at www.sciencedirect.com
ScienceDirect
Trans. Nonferrous Met. Soc. China 31(2021) 2615−2625
Transactions of Nonferrous Metals Society of China
www.tnmsc.cn

Effects of annealing on mechanical properties and degradation behavior of biodegradable JDBM magnesium alloy wires

Yuan TIAN[1], Hong-wei MIAO[1], Jia-lin NIU[1], Hua HUANG[1],
Bin KANG[2], Hui ZENG[2], Wen-jiang DING[1,2], Guang-yin YUAN[1,2]

1. National Engineering Research Center of Light Alloy Net Forming and
State Key Laboratory of Metal Matrix Composite, Shanghai Jiao Tong University, Shanghai 200240, China;
2. National & Local Joint Engineering Research Center of Orthopedic Biomaterials,
Department of Bone & Joint Surgery, Peking University Shenzhen Hospital, Shenzhen 518036, China

Received 18 November 2020; accepted 8 May 2021

Abstract: Mg−Nd−Zn−Zr magnesium alloy (JDBM) has been studied widely as biodegradable medical material. To process high quality JDBM wires, effects of annealing on the mechanical properties and degradation behavior after drawing were studied by microscopic observations, tensile and immersion tests. The as-extruded wires with a diameter of 3 mm could be drawn up to 9 passes without annealing until 125% cumulative drawing deformation. Complete recrystallization occurred after annealing at 325 °C for 30 min, 350 °C for 5 min or 450 °C for 3 min, respectively. Room temperature tensile tests and simulated body fluid immersion tests showed that annealing at slightly elevated temperature for short time could obtain better properties due to the finer grain size and more dispersive distribution of precipitates. For this study, annealing at 350 °C for 5 min is the best parameters which can be utilized to further fabricate fine wires.

Key words: Mg−Nd−Zn−Zr alloy; drawing; annealing; mechanical properties; corrosion rate

1 Introduction

Magnesium alloys are promising candidates for clinical implants due to their good bio-compatibility and biodegradation in vivo. They are able to replace traditional bio-inert medical metallic materials, such as stainless steel, and titanium alloy, in the fields of orthopedic implants, vascular stents and other medical implants in the future [1−6]. Magnesium alloy wires can be used to fabricate products, such as staples and intramedullary nails, which exhibit a wide range of applications. In addition, they can also be made into vascular stents and medical cables by weaving. At present, related medical implants using stainless steel and titanium alloy wires have been well developed [7]. However, the use of magnesium alloy wires can avoid the risk of secondary surgery or long-term immune response. Therefore, the manufacture of wires with high quality becomes very important for magnesium alloy applications as biodegradable material.

For the manufacture of magnesium alloy wires, cold drawing with following annealing has been applied in a large number of studies. And various kinds of magnesium alloy wires with excellent mechanical properties substantially meeting the requirements for biomedical applications have been prepared by this kind of method [8−12]. However, the corrosion rate of the existing magnesium alloy

Corresponding author: Hua HUANG, Tel: +86-21-34203051, Fax: +86-21-34202794, E-mail: huangh@sjtu.edu.cn;
Hui ZENG, E-mail: zenghui_36@163.com;
Guang-yin YUAN, Tel: +86-21-34203051, Fax: +86-21-34202794, E-mail: gyyuan@sjtu.edu.cn
DOI: 10.1016/S1003-6326(21)65680-7

wires is still relatively fast, which greatly restricts its application in the field of medical devices. Because most of these researches mainly focus on the optimization of mechanical properties, the commercial magnesium alloys used in their studies usually have relatively fast degradation rate and poor biocompatibility. Furthermore, the effect of fabrication process on the degradation rate of magnesium alloy wires is usually ignored. Therefore, in order to obtain the biomedical magnesium alloy wires with excellent mechanical properties, corrosion behavior as well as biocompatibility, the processing parameters and the type of the alloy adopted are crucial.

Based on the previous studies, the main problems that restrict the medical application of magnesium alloys are the poor plastic deformability and the fast corrosion rate. A lot of researches have been done on these two major issues since the beginning of 21st century [6,13−16], and alloying with rare earth elements (RE) has been proved to be effective. Adding appropriate rare earth element and contents into magnesium alloys could not only improve the mechanical properties, but also reduce the degradation rate [17]. At present, biodegradable vascular stent developed on the basis of rare earth magnesium alloy WE43 has been used clinically in Europe. Mg−Nd−Zn−Zr biodegradable magnesium alloy (JDBM) developed by our research group has also been confirmed to possess high mechanical properties, good biocompatibility and favorable uniform degradation behavior in simulated body fluid (SBF) [8,18−23]. The relative researches confirmed that JDBM alloy is one of the candidate materials for biomedical applications. In this study, JDBM alloy was chosen for drawing in order to process biodegradable wires for further implants fabrication.

The purpose of this study was to find proper annealing parameters which can be used for high quality JDBM wires processing. The JDBM wire with the diameter of about 3.0 mm was firstly fabricated by hot extrusion and then processed by multi-pass drawing without annealing. The maximum number of the drawing passes is confirmed by checking the surface quality of the wires. After that, wires with the maximum cold drawing passes were chosen for annealing to study the effects of annealing parameters on the microstructure, mechanical and corrosion properties.

2 Experimental

2.1 Wires preparation

In this study, a set of JDBM (Mg−2.1Nd−0.2Zn−0.5Zr, wt.%) [24] samples were prepared with different kinds of methods. Samples for drawing were prepared by hot extrusion: the diameter of the JDBM samples for extrusion was 20.0 mm, the hot extrusion temperature was 380 °C, and the extrusion speed was 1.5 mm/s. The dimension of the JDBM samples after extrusion was 3.0 mm in diameter. Some of the as-extruded samples were used for the cold drawing, and the others were used for microstructure and properties characterization.

The multi-pass cold drawing was adopted as follows: the as-extruded wires were cold drawn by sequentially arranged molds in the order of 2.8, 2.7, 2.6, up to 1.9 mm in diameter. There was no annealing treatment between these passes. The drawing speed was about 100 mm/s. After drawing, some of the samples were annealed at different temperatures from 325 to 450 °C for different time to determine the optimal annealing parameters.

2.2 Microstructure and hardness analysis

The microstructure of the JDBM wires was characterized primarily by optical microscopy (OM). The samples were polished and etched by a mixed solution containing 1 g of oxalic acid, 1 mL of nitric acid, 1 mL of acetic acid, and 150 mL of distilled water.

The Vickers microhardness tester was used to characterize the hardness of the samples. The test force was 0.98 N. The cross-section of the wires was used for hardness test and these samples were prepared according to metallographic standards. After determining the optimal annealing parameters by hardness change, scanning electron microscope (SEM), energy dispersive X-ray spectroscope (EDS) and electron backscattered diffraction (EBSD) technologies were used to further study the microstructure of the samples with the optimal annealing parameters.

2.3 Mechanical and degradation properties tests

Room temperature tensile test was used to characterize the yield strength, tensile strength and elongation of the samples by using a Zwick/Roell

Z100 standard tensile testing machine. The initial tensile strain rate was 1×10^{-3} s^{-1}.

Corrosion resistance was mainly characterized by immersion experiment in simulated body fluid. In this study, Hank's solution was chosen as simulated human body fluid [25]. The amount of solution used in the experiment was based on the immersion corrosion standard ASTM G31—72 [26]. Corrosion resistance of the sample was measured through hydrogen evolution during immersion test.

3 Results

3.1 Determination of drawing passes

Figure 1 shows the surface morphologies of the wires after 9 and 10 passes cold drawing. Figure 1(a) shows the macrophotograph of the wires, Figs. 1(b) and (c) reveal the corresponding detailed SEM images. The wires after 9 passes cold drawing basically have no obvious defects. However, after 10 passes cold drawing, many defects can be found although there are no crack trails. Therefore, samples with 9 passes cold drawing were chosen for later research on annealing. The initial dimension of the samples was about 3 mm in diameter, and the final dimension was about 2 mm in diameter. Hence, the cumulative drawing deformation was 125%.

3.2 Hardness and microstructural evolution

After annealing at 325, 350 and 450 °C, the hardness evolution is shown in Fig. 2. The hardness of the as-extruded JDBM wires is (63.7±0.3) HV, which is (74.3±0.9) HV for the as-drawn wires. Therefore, the hardness of the wires increases significantly due to work hardening after cold drawing, and the increment is about 16.6%. During annealing, the hardness of the wires increased firstly and then decreased for the samples annealed at 325 °C. However, for the other two groups of samples annealed at 350 or 450 °C, hardness of the wires decreased gradually. Furthermore, significant hardness decreases was found for the samples annealed at 325 °C for 30 min, 350 °C for 5 min and 450 °C for 3 min, respectively. These annealing conditions were considered as proper parameters for eliminating the work hardening.

The optical microstructures of the samples annealed with these proper parameters and the as-extruded as well as as-drawn samples were characterized and shown in Fig. 3, which confirmed that the stretched grains for the as-drawn sample

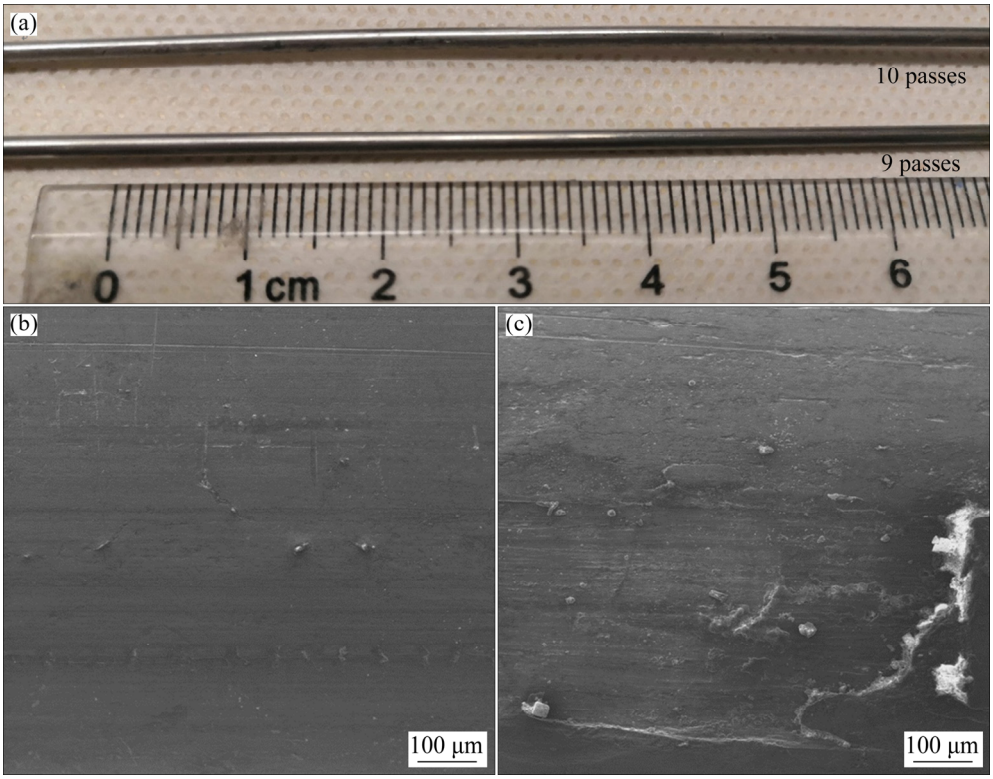

Fig. 1 Surface images of wires after cold drawing: (a) Macrograph; (b) SEM image after 9 passes cold drawing; (c) SEM image after 10 passes cold drawing

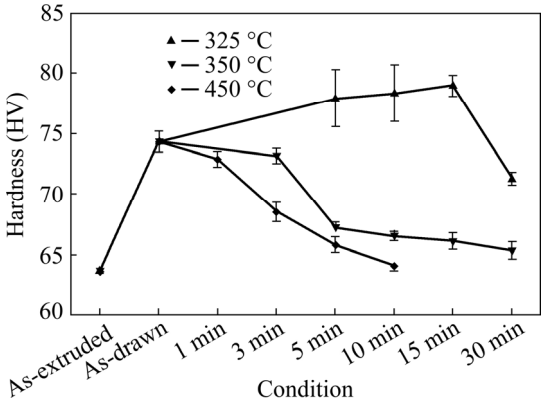

Fig. 2 Hardness evolution during annealing at different temperatures

became equiaxed again after annealing with these optimal parameters. It could be considered that recrystallization was substantially completed at these optimal annealing parameters. Therefore, the proper annealing parameters for further study were determined to be at 325 °C for 30 min, 350 °C for 5 min and 450 °C for 3 min, and hereafter these samples are denoted as 325-30, 350-5 and 450-3, respectively.

Figure 4 shows the microstructures of the cross-sections of the as-extruded and annealed samples which were characterized by SEM. Some characteristics of the annealed JDBM magnesium alloy wires with a diameter of 2.0 mm can be found: (1) the grain size of annealed samples is smaller compared to that of the as-extruded samples; (2) the second phase particles are uniformly dispersed in the cross-section. However, the samples after annealing seem to have more secondary phases, and 325-30 sample seems to have the largest amount of the secondary phases.

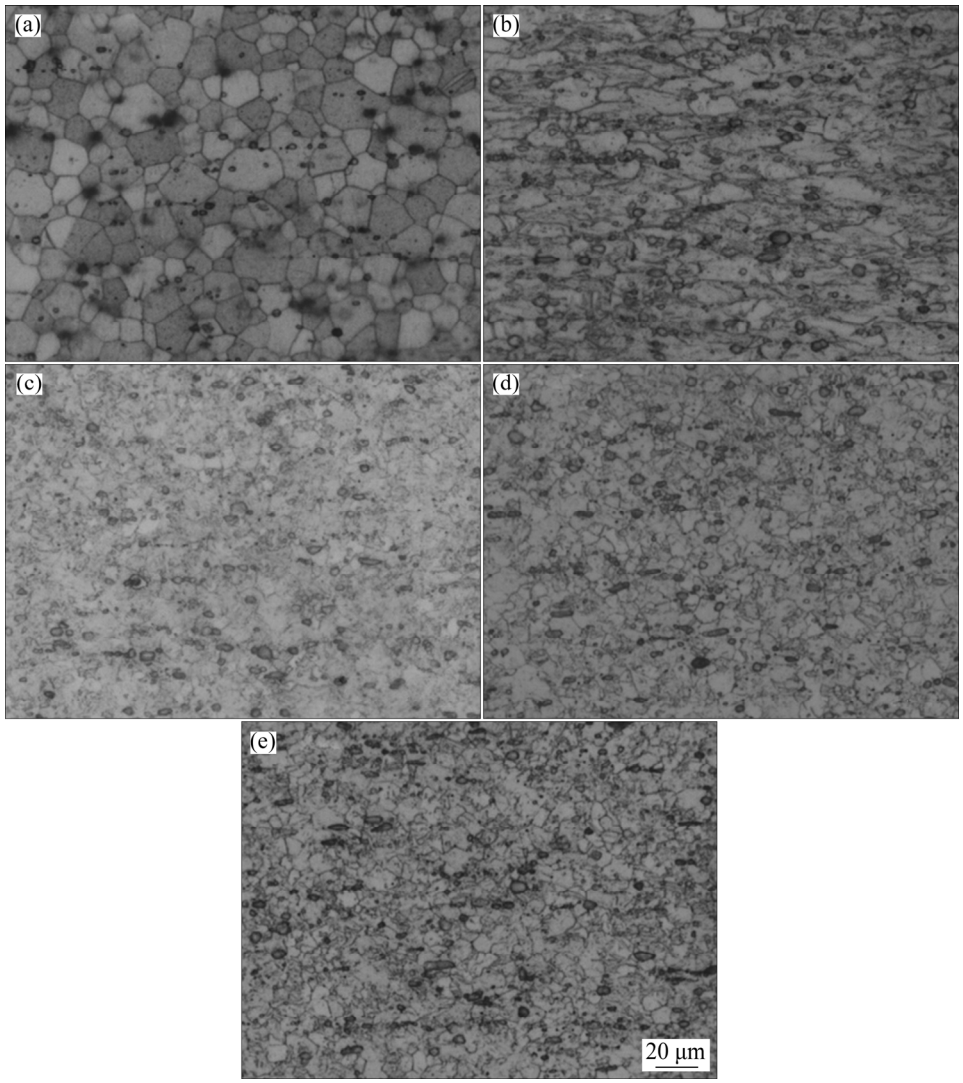

Fig. 3 Optical microstructures before and after cold drawing and different annealing treatments: (a) As-extruded; (b) As-drawn; (c) 325-30; (d) 350-5; (e) 450-3

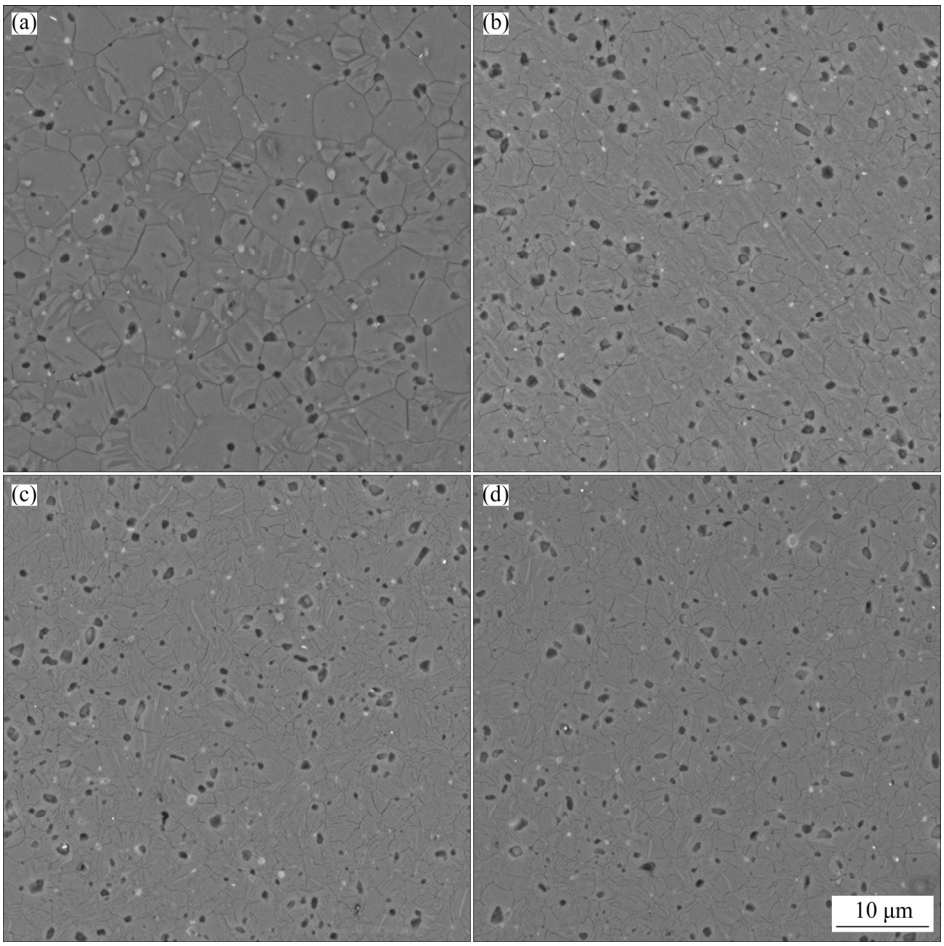

Fig. 4 SEM images of cross-sections for as-extruded and annealed samples: (a) As-extruded; (b) 325-30; (c) 350-5; (d) 450-3

The statistical results of the secondary phase content are shown in Fig. 5. The contents of secondary phase for the samples of as-extruded, 325-30, 350-5, and 450-3 samples are (5.1±1.0), (9.8±1.0), (6.9±1.4), and (6.5±1.0) vol.%, respectively. Therefore, the volume fraction of secondary phases will increase through drawing and annealing treatments. The increment for 325-30 sample is significantly greater than 350-5 and 450-3 samples, and the latter two show very similar microstructure.

The average grain sizes of the samples were calculated by the interception method. The statistical results are shown in Fig. 6. It can be found that the average grain sizes of the as-extruded, 325-30, 350-5, and 450-3 samples are (4.2±0.5), (3.1±0.2), (2.7±0.3), and (2.6±0.3) μm, respectively. In addition, the average grain sizes of the annealed samples do not change significantly with the annealing temperature, and all of them are smaller than that of the as-extruded sample. Therefore, all of the annealed samples have not gone through significant grain growth after annealing with those proper parameters, which lead to the refined grains.

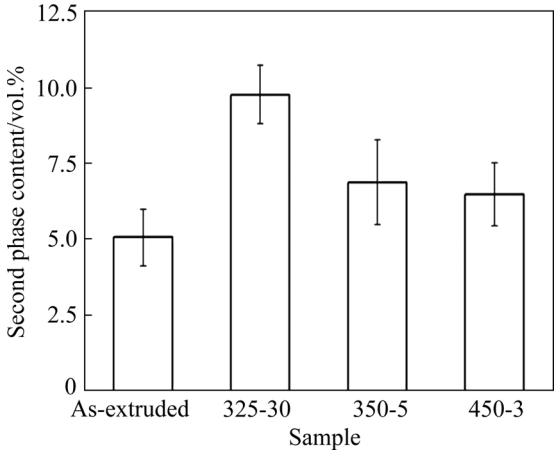

Fig. 5 Secondary phase contents for as-extruded, 325-30, 350-5, and 450-3 samples

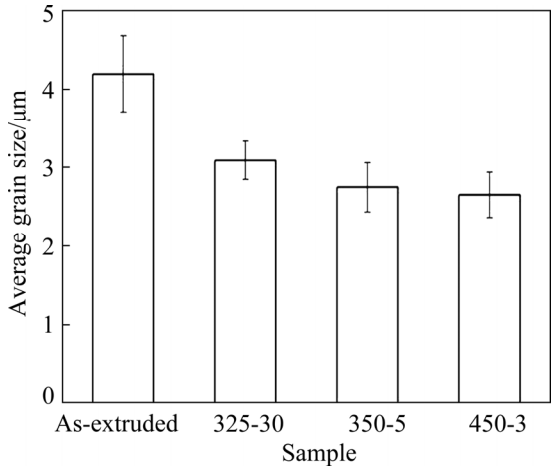

Fig. 6 Average grain sizes for as-extruded, 325-30, 350-5, and 450-3 samples

Based on the above optical and SEM characterization results about the microstructure, the 325-30 sample has the highest secondary phase content and average grain size, which imply inferior properties. Therefore, EBSD method was only used to reveal the orientation information of the grains for the as-extruded, 350-5 and 450-3 samples. Different types of grain boundaries are shown in Fig. 7 by different colors. After annealing, the $\{10\bar{1}2\}$ twins disappear and the amount of low-angle grain boundary (LAGB) decreases, which can be considered as an evidence of microstructure evolution from deformed grain to recrystallization. In Fig. 8, the results of texture clearly show that annealing at 350 and 450 °C can greatly reduce the intensity of basal texture.

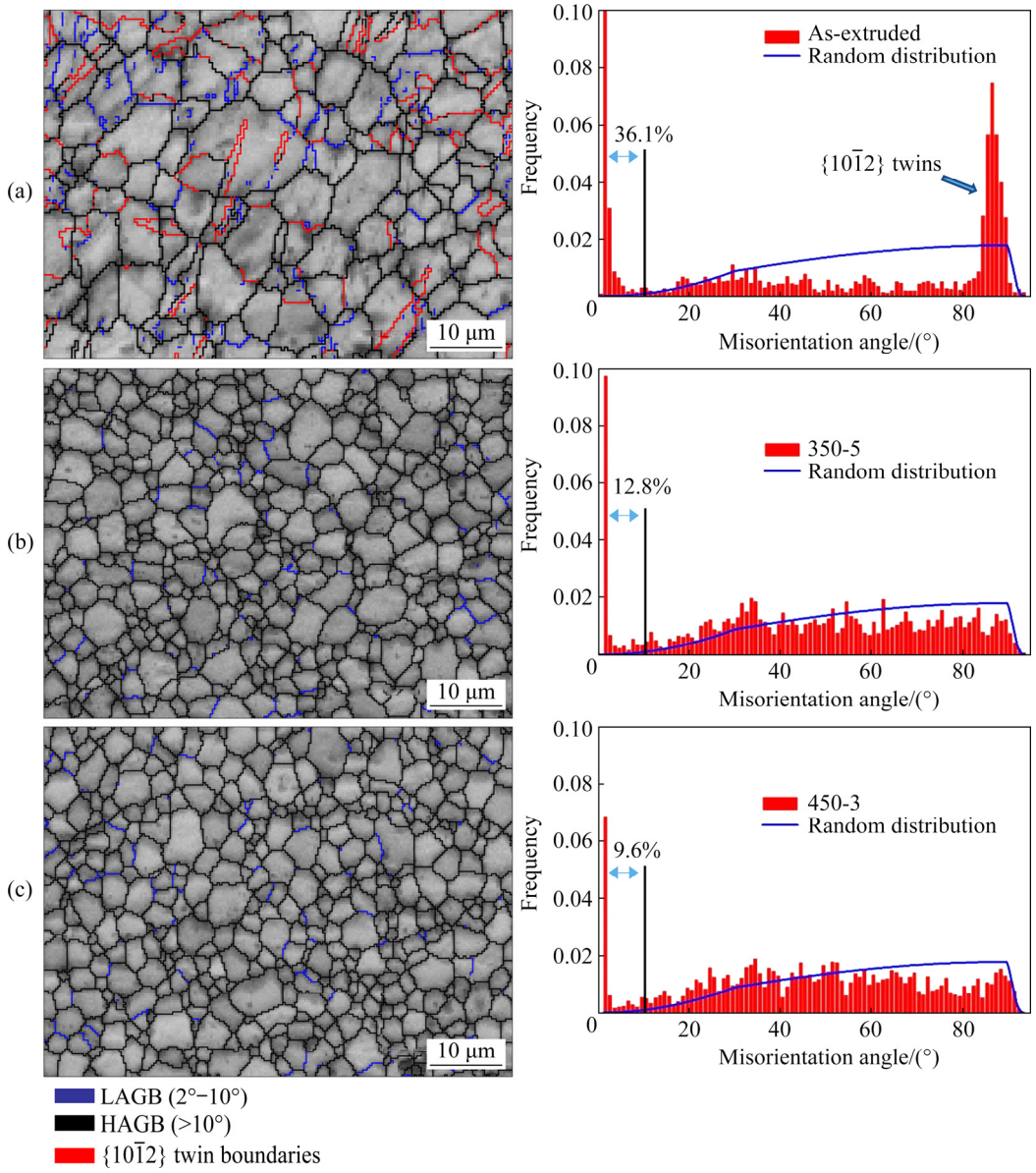

Fig. 7 Grain boundaries information for as-extruded (a), 350-5 (b), and 450-3 (c) samples

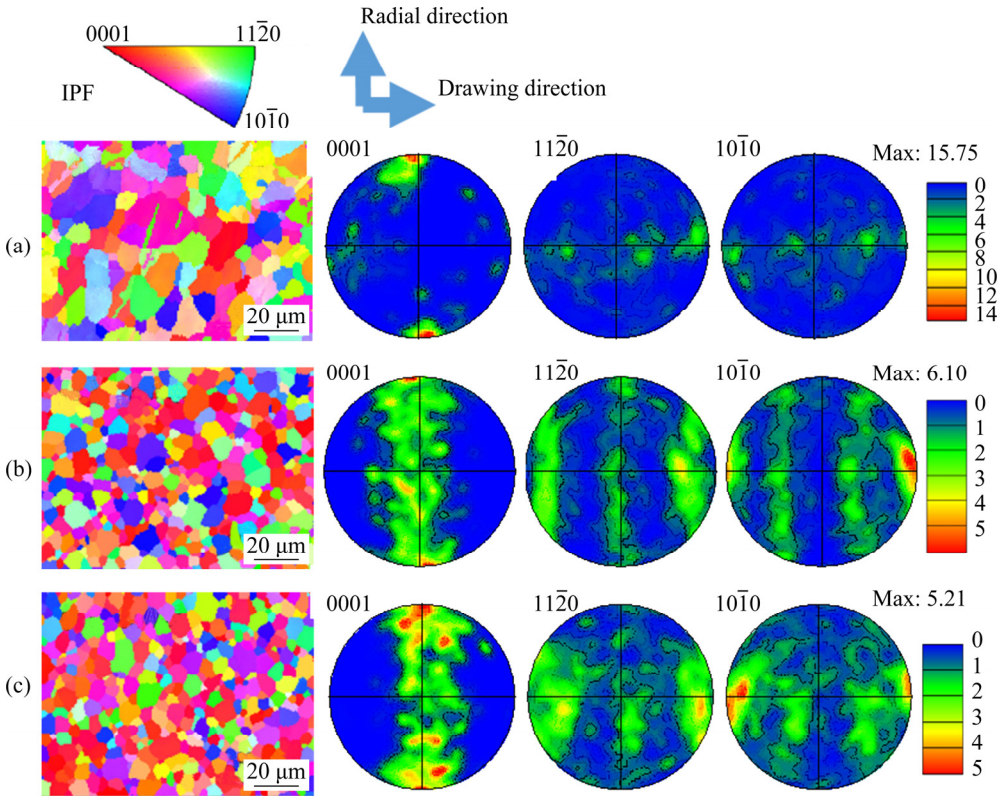

Fig. 8 Textures for as-extruded (a), 350-5 (b), and 450-3 (c) samples

3.3 Mechanical properties

Figure 9 shows the representative room temperature tensile stress−strain curves for the samples under different conditions. The yield strength for the as-extruded wire is about 151 MPa, which is about 313 MPa for the as-drawn wires. In addition, the as-drawn sample exhibits the highest tensile strength, but there is no obvious yielding due to the cold drawing and its elongation is only about 6.3%. Consequently, the wires become unsuitable for further cold drawing due to the dramatically decreased elongation. The annealed samples have obvious yielding phenomenon. After annealing, there is a huge improvement for elongation when the annealing temperature rises from 325 to 350 °C. However, when the temperature rises from 350 to 450 °C, the elongation decreases slightly with a little increase in strength. The 350-5 sample has 257.5 MPa in yield strength, 280.2 MPa in tensile strength and 18.4% in elongation.

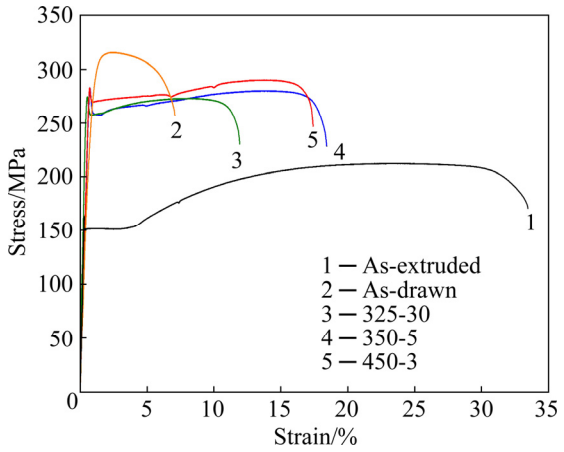

Fig. 9 Representative room temperature tensile stress−strain curves of different samples

3.4 Corrosion behavior

Figure 10 shows the hydrogen evolution curves for the studied samples with different immersion time in Hank's solution at 37 °C. The curves for the hydrogen evolution and immersion time of all samples are basically linear. Therefore, it can be considered that the reaction between the sample and the etching solution is stable during the corrosion process. Corrosion rate of the group of samples annealed at 325 °C for 30 min is significantly faster than that of the other annealed samples. In addition, the amount of hydrogen evolution of the as-drawn, 350-5 and 450-3 samples is very close. There is no significant difference in the amount of hydrogen evolution between the three groups when they are immersed for 240 h. Therefore,

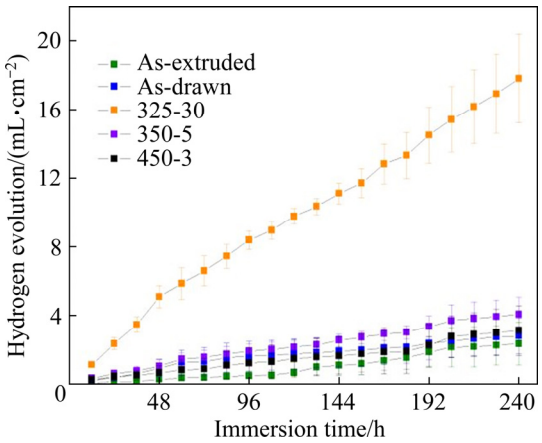

Fig. 10 Hydrogen evolution for JDBM wires before and after cold drawing with different annealing treatments

it can be considered that the corrosion behavior of the sample will not be sacrificed obviously after cold drawing and then annealing with optimal parameters. The corrosion rate of 350-5 sample can be calculated from the hydrogen evolution in Fig. 10, which is about 0.42 mm/a.

For biodegradable materials, in addition to the suitable degradation rate, they are also supposed to exhibit sufficient mechanical properties and maintain a certain shape during the service period. In this study, the surface morphologies after immersion for the samples with and without corrosion products were studied, which are shown in Fig. 11. The micro-corrosion morphologies of the studied samples are nearly the same, the corrosion products are scattered and accumulated on the surface of the samples, and all the samples are corroded with some deep traces. Among all the samples, the corrosion product of the 325-30 sample is much more than that of others, which is coincided with the fast corrosion rate. After washing off the corrosion products, small and scattered pits appear on all samples. And the corrosion pits of 325-30 sample are much bigger, which corresponds well with the corrosion rate. The corrosion pits of 450-3 sample are slightly smaller than those of 350-5 sample, indicating the better corrosion resistance.

4 Discussion

4.1 Optimization of annealing parameters

Annealing is a traditional heat treatment method for cold deformation. In this study, the purpose of annealing is to eliminate the effect of cold deformation through recovery and recrystallization, and then make that the wires could be drawn again. Finishing recrystallization and controlling grain growth are set to be the target of annealing. The metallographic observation and

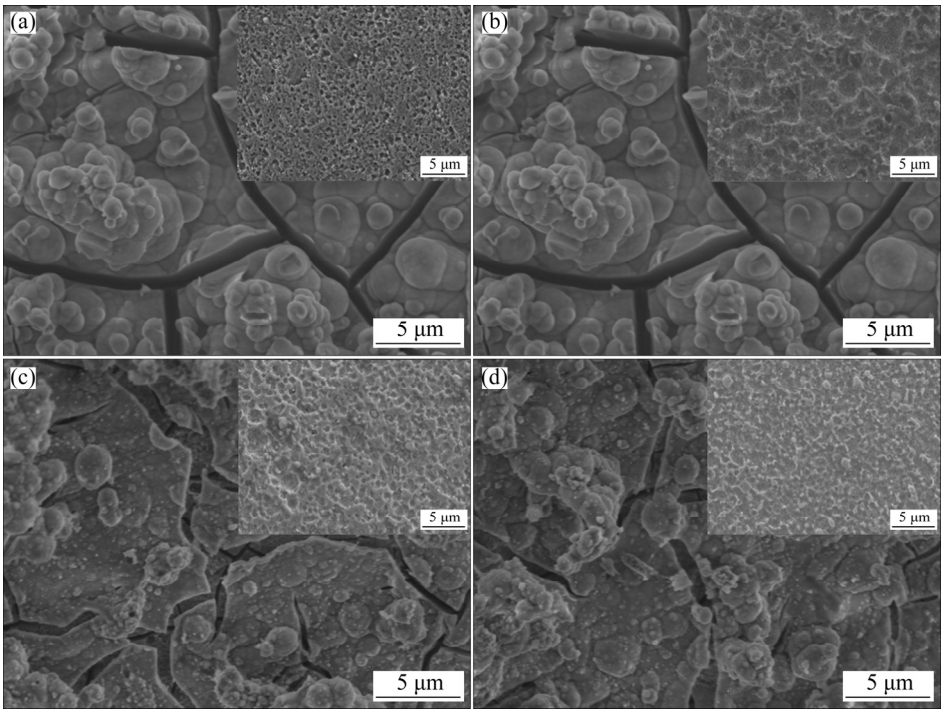

Fig. 11 Surface morphologies for samples after immersion with inserted corresponding surface images after removing corrosion products: (a) As-extruded; (b) 325-30; (c) 350-5; (d) 450-3

hardness tests results of the samples under different annealing conditions are vital evidence for determining the appropriate annealing parameters. After cold drawing deformation, the grains usually show a stretched morphology due to the abundant dislocations motion. Meanwhile, due to a large number of dislocations in the sample, interactive entanglement of the dislocations will increase the hardness and yield strength (YS) of the alloy. During annealing, the microstructure of the alloy will gradually go through recovery, recrystallization and grain growth. Therefore, appropriate annealing temperature and time could be roughly estimated based on the changing trend of the metallographic and hardness of the sample. In this study, after annealing under the conditions of 325-30, 350-5 and 450-3 samples, the hardness of the samples decreased obviously (Fig. 2) and the stretched grains became equiaxed grains (Fig. 3), both of which confirmed that the target of annealing was achieved. Therefore, 325-30, 350-5 and 450-3 samples were considered to be appropriate annealing conditions.

4.2 Effects of annealing on mechanical properties and corrosion behavior

In this study, the hardness of JDBM wires after 9 passes drawing increased from (63.7±0.3) to (74.3±0.9) HV due to work hardening, increased by 16.6% (Fig. 2). The YS increased from 151 to 313 MPa correspondingly, increased by 107% (Fig. 9). Consequently, the elongation decreased dramatically and then the wires became not suitable for drawing (Fig. 1). After annealing under the conditions of 325-30, 350-5 and 450-3 samples, all the wires could be cold drawn again. Moreover, the annealing treatment from 325-30 to 350-5 sample, elongation and corrosion performance were improved significantly. There is almost no difference in grain size between them (Fig. 6), while a huge difference exists in secondary phase content (Fig. 5). The main secondary phase in JDBM alloy is $Mg_{12}Nd$, and the proper solid solution temperature is 540 °C [24,27]. Since the annealing temperature is lower than the solid solution temperature, secondary phase precipitation will occur during this heat treatment. Therefore, during the annealing, there are two competing mechanisms: recrystallization and secondary phase precipitation. Both mechanisms will consume the energy that accumulates during the cold deformation. At higher annealing temperatures, recrystallization is more rapid, while precipitation of the second phase is slower due to the decrease of difference between the annealing and solid solution temperatures. Finally, higher annealing temperature with short time allows recrystallization to be completed quickly, contributing to finer grains and less precipitation of the secondary phase, so better elongation can be obtained without sacrifice of strength. On the contrary, lower annealing temperature with long time increases the tendency of the secondary phase precipitation, leading to slightly coarser grains and more precipitates, and the elongation is lower. In addition, the two competing mechanisms of recrystallization and secondary phase precipitation also have different effects on hardness. The former leads to the hardness decreasing, while the later causes hardness increasing. However, since the secondary phase precipitation is limited by the alloying concentration, it can only occur at the early stage of annealing. In this study, the hardness of 325 °C sample increases as the time increases at the early stage of annealing mainly due to the secondary phase precipitation. The secondary phase content for 325 °C sample is the largest (Fig. 5), which is the best evidence. Therefore, higher annealing temperature with short time is beneficial to better mechanical properties, especially for elongation that is critical for further cold drawing. In terms of corrosion behavior, since the precipitation of the secondary phase is more likely to cause galvanic corrosion, which accelerates the corrosion rate, the wires annealed at a higher temperature for a short time exhibit a slower corrosion rate (Fig. 10).

However, since the JDBM wires are manufactured by hot extrusion and already have secondary phase precipitation, the secondary phase precipitation is limited by the alloying concentration. Therefore, with further increase in the annealing temperature to 450 °C, there is no obvious difference for the microstructure and properties. Therefore, properly increasing annealing temperature is beneficial to obtaining high quality wires with good mechanical properties and corrosion behavior, and in this study the best annealing condition is at 350 °C for 5 min.

5 Conclusions

(1) For JDBM magnesium alloy, under the conditions of this experiment, cold drawing without annealing can be carried out up to 9 passes, reaching the cumulative deformation of 125%. After cold drawing by multiple passes, the grains are obviously elongated in the drawing direction.

(2) Recrystallization and precipitation of the secondary phase occur simultaneously during annealing. The lower annealing temperature and longer annealing time lead to more precipitates of secondary phases. The recrystallization of the JDBM magnesium alloy could be finished within 30 min at 325 °C, 5 min at 350 °C, and 3 min at 450 °C.

(3) After the comprehensive analysis of mechanical properties and corrosion behavior, it is considered that the optimum annealing strategy for JDBM multi-pass drawing is annealing at slightly elevated temperature with short time. In this case, the recommended annealing parameters are at 350 °C for 5 min, by which the wires have 257.5 MPa in yield strength, 280.2 MPa in tensile strength, 18.4% in elongation and 0.42 mm/a in corrosion rates in Hank's solution.

Acknowledgments

This work was financially supported by the National Natural Science Foundation of China (No. U1804251), the Shanghai Municipal Commission of Economy and Information, China (No. GYQJ-2019-1-27), the Science and Technology Commission of Shanghai Municipality, China (Nos. 18441908000, 19441906300, 19441913400), the Shenzhen's Three Renowned Project, China (No. SZSM201612092), and the Shanghai Jiao Tong University Medical-engineering Cross Fund, China (No. YG2019ZDA02).

References

[1] STAIGER M P, PIETAK A M, HUADMAI J, DIAS G. Magnesium and its alloys as orthopedic biomaterials: A review [J]. Biomaterials, 2006, 27: 1728−1734.

[2] WITTE F. The history of biodegradable magnesium implants: A review [J]. Acta Biomaterialia, 2010, 6: 1680−1692.

[3] CHEN Yong-jun, XU Zhi-gang, SMITH C, SANKAR J. Recent advances on the development of magnesium alloys for biodegradable implants [J]. Acta Biomaterialia, 2014, 10: 4561−4573.

[4] CAI Chang-hong, ALVES M M, SONG Ren-bo, WANG Yong-jin, LI Jing-yuan, MONTEMOR M F. Non-destructive corrosion study on a magnesium alloy with mechanical properties tailored for biodegradable cardiovascular stent applications [J]. Journal of Materials Science & Technology, 2021, 66: 128−138.

[5] ZHANG Yi, TAN Li-li, WANG Qing-chuan, GAO Ming, ETIM I P, YANG Ke. Effects of microstructure on the torsional properties of biodegradable WE43 Mg alloy [J]. Journal of Materials Science & Technology, 2020, 51: 102−110.

[6] TAN Li-li, YU Xiao-ming, WAN Peng, YANG Ke. Biodegradable materials for bone repairs: A review [J]. Journal of Materials Science & Technology, 2013, 29: 503−513.

[7] GBUR J L, LEWANDOWSKI J J. Fatigue and fracture of wires and cables for biomedical applications [J]. International Materials Review, 2016, 61: 231−314.

[8] BAI Jing, YIN Ling-ling, LU Ye, GAN Yi-wei, XUE Feng, CHU Cheng-lin, YAN Jing-li, YAN Kai, WAN Xiao-feng, TANG Zhe-jun. Preparation, microstructure and degradation performance of biomedical magnesium alloy fine wires [J]. Progress in Natural Science: Materials International 2014, 24: 523−530.

[9] SEITZ J M, WULF E, FREYTAG P, BORMANN D, BACH F W. The manufacture of resorbable suture material from magnesium [J]. Advanced Engineering Materials, 2010, 12: 1099−1105.

[10] SEITZ J M, UTERMÖHLEN D, WULF E, KLOSE C, BACH F W. The manufacture of resorbable suture material from magnesium — Drawing and stranding of thin wires [J]. Advanced Engineering Materials, 2011, 13: 1087−1095.

[11] SUN Liu-xia, BAI Jing, YIN Ling-ling, GAN Yi-wei, XUE Feng, CHU Cheng-lin, YAN Jing-lin, WAN Xiao-feng, DING Hong-yan, ZHOU Guang-hong. Effect of annealing on the microstructures and properties of cold drawn Mg alloy wires [J]. Materials Science and Engineering A, 2015, 645: 181−187.

[12] SHAN Zhao-hui, BAI Jing, FAN Jian-feng, WU Hong-fei, ZHANG Hua, ZHANG Qiang, WU Yu-cheng, LI Wei-guo, DONG Hong-biao, XU Bing-she. Exceptional mechanical properties of AZ31 alloy wire by combination of cold drawing and EPT [J]. Journal of Materials Science & Technology, 2020, 51: 111−118.

[13] DING Yun-fei, WEN Cui-e, HODGSON D P, LI Yun-cang. Effects of alloying elements on the corrosion behavior and biocompatibility of biodegradable magnesium alloys: A review [J]. Journal of Materials Chemistry B, 2014, 2: 1912−1933.

[14] AGARWAL S, CURTIN J, DUFFY B, JAISWAL S. Biodegradable magnesium alloys for orthopaedic applications: A review on corrosion, biocompatibility and surface modifications [J]. Materials Science and Engineering C, 2016, 68: 948−963.

[15] LI Xia, LIU Xiang-mei, WU Shui-lin, YEUNG K W K, ZHENG Yu-feng, CHU P K. Design of magnesium alloys with controllable degradation for biomedical implants: From bulk to surface [J]. Acta Biomaterialia, 2016, 45: 2−30.

[16] CAI Shu-hua, LEI Ting, LI Nian-feng, FENG Fang-fang. Effects of Zn on microstructure, mechanical properties and corrosion behavior of Mg−Zn alloys [J]. Materials Science and Engineering C, 2012, 32: 2570−2577.
[17] ROKLIN L L. Magnesium alloy containing rare-earth metals: Structures and properties [M]. New York: Taylor & Francis, 2002.
[18] ZHANG Xiao-bo, YUAN Guang-yin, MAO Lin, NIU Jia-lin, DING Wen-jiang. Biocorrosion properties of as-extruded Mg–Nd–Zn–Zr alloy compared with commercial AZ31 and WE43 alloys [J]. Materials Letters, 2012, 66: 209−211.
[19] GUAN Xing-min, XIONG Mei-ping, ZENG Fei-yue, XU Bin, YANG Ling-di, GUO Han, NIU Jia-lin, ZHANG Jian, CHEN Chen-xin, PEI Jia, HUANG hua, YUAN Guang-yin. Enhancement of osteogenesis and biodegradation control by brushite coating on Mg−Nd−Zn−Zr alloy for mandibular bone repair [J]. ACS Applied Materials & Interfaces, 2014, 6: 21525−21533.
[20] MAO Lin, SHEN Li, CHEN Jia-hui, WU Yu, KWAK M, LU Yao, XUE Qiong, PEI Jia, ZHANG Lei, YUAN Guang-yin, FAN Rong, GE Jun-bo, DING Wen-jiang. Enhanced bioactivity of Mg−Nd−Zn−Zr alloy achieved with nanoscale MgF_2 surface for vascular stent application [J]. ACS Applied Materials & Interfaces, 2015, 7: 5320−5330.
[21] JIN Liang, CHEN Chen-xin, JIA Gao-zhi, LI Yu-tong, ZHANG Jian, HUANG Hua, KANG Bin, YUAN Guang-yin, ZENG Hui, CHEN Tong-xin. The bioeffects of degradable products derived from a biodegradable Mg-based alloy in macrophages via heterophagy [J]. Acta Biomaterialia, 2020, 106: 428−438.
[22] ZHANG Jian, LI Hai-yan, WANG Wu, HUANG Hua, PEI Jia, QU Hai-yun, YUAN Guang-yin, LI Yong-dong. The degradation and transport mechanism of a Mg-Nd-Zn-Zr stent in rabbit common carotid artery: A 20-month study [J]. Acta Biomaterialia, 2018, 69: 372−384.
[23] QIN Hui, ZHAO Yao-chao, AN Zhi-quan, CHENG Meng-qi, WANG Qi, CHENG Tao, WANG Qiao-jie, WANG Jia-xing, JIANG Yao, ZHANG Xiao-long, YUAN Guang-yin. Enhanced antibacterial properties, biocompatibility, and corrosion resistance of degradable Mg−Nd−Zn−Zr alloy [J]. Biomaterials, 2015, 53: 211−220.
[24] ZHANG Xiao-bo, YUAN Guang-yin, MAO Lin, NIU Jia-lin, FU Peng-huai, DING Wen-jiang. Effects of extrusion and heat treatment on the mechanical properties and biocorrosion behaviors of a Mg−Nd−Zn−Zr alloy [J]. Journal of the Mechanical Behavior of Biomedical Materials, 2012, 7: 77−86.
[25] HILTZ J, TROPE M. Vitality of human lip fibroblasts in milk, Hanks balanced salt solution and Viaspan storage media [J]. Endodontics & Dental Traumatology, 1991, 7: 69−72.
[26] ASTM-G31—72. Annual book of ASTM standards [S]. Philadelphia, Pennsylvania, USA, 2004.
[27] FU Peng-huai, PENG Li-ming, JIANG Hai-yan, CHANG Jian-wei, ZHAI Chun-quan. Effects of heat treatments on the microstructures and mechanical properties of Mg−3Nd−0.2Zn−0.4Zr (wt.%) alloy [J]. Materials Science and Engineering A, 2008, 486: 183−192.

退火工艺对生物可降解 JDBM 镁合金丝材力学性能与降解行为的影响

田 圆[1]，苗宏卫[1]，牛佳林[1]，黄 华[1]，康 斌[2]，曾 晖[2]，丁文江[1,2]，袁广银[1,2]

1. 上海交通大学 轻合金精密成型国家工程研究中心，金属基复合材料国家重点实验室，上海 200240；
2. 北京大学深圳医院 骨科和关节外科，生物材料国家地方联合工程研究中心，深圳 518036

摘 要：Mg−Nd−Zn−Zr 生物可降解镁合金(JDBM)作为一种生物医用材料得到了广泛的关注和研究。为了加工高质量的 JDBM 丝材，通过显微镜观察、拉伸试验和浸没试验研究退火对拉拔后 JDBM 线材力学性能和降解行为的影响。对于直径为 3 mm 的挤压态合金丝，室温拉拔加工最多可连续进行 9 道次而无需退火，累积拉伸变形为 125%。对拉拔后的合金丝分别在 325 °C 退火 30 min、350 °C 退火 5 min 或 450 °C 退火 3 min 后发生完全再结晶。室温拉伸试验和模拟体液浸没试验结果表明，在稍高的温度下进行短时间退火后，由于晶粒细小和沉淀物的分散分布，合金丝可以获得更好的性能。在本研究中，在 350 °C 下退火 5 min 是拉拔后最佳的退火参数，可用于进一步制造更细的合金丝材。

关键词：Mg−Nd−Zn−Zr 合金；拉拔；退火；力学性能；腐蚀速率

(Edited by Wei-ping CHEN)